Human ornithine aminotransferase complexed with L-canaline and gabaculine: structural basis for substrate recognition

Sapan A Shah[1], Betty W Shen[1] and Axel T Brünger[1,2]*

Background: Ornithine aminotransferase (OAT) is a 45 kDa pyridoxal-5′-phosphate (PLP)-dependent enzyme that catalyzes the conversion of L-ornithine and 2-oxoglutarate to glutamate-δ-semialdehyde and glutamic acid, respectively. In humans, loss of OAT function causes an accumulation of ornithine that results in gyrate atrophy of the choroid and retina, a disease that progressively leads to blindness. In an effort to learn more about the structural basis of this enzyme's function, we have determined the X-ray structures of OAT in complex with two enzyme-activated suicide substrates: L-canaline, an ornithine analog, and gabaculine, an irreversible inhibitor of several related aminotransferases.

Results: The structures of human OAT bound to the inhibitors gabaculine and L-canaline were solved to 2.3 Å at 110K by difference Fourier techniques. Both inhibitors coordinate similarly in the active site, binding covalently to the PLP cofactor and causing a 20° rotation in the cofactor tilt relative to the ligand-free form. Aromatic–aromatic interactions occur between the bound gabaculine molecule and active-site residues Tyr85 and Phe177, whereas Tyr55 and Arg180 provide specific contacts to the α-amino and carboxyl groups of L-canaline.

Conclusions: The OAT–L-canaline complex structure implicates Tyr55 and Arg180 as the residues involved in coordinating with the natural substrate ornithine during normal enzyme turnover. This correlates well with two enzyme-inactivating point mutations associated with gyrate atrophy, Tyr55→His and Arg180→Thr. The OAT–gabaculine complex provides the first structural evidence that the potency of the inhibitor is due to energetically favorable aromatic interactions with residues in the active site. This aromatic-binding mode may be relevant to structure-based drug design efforts against other ω-aminotransferase targets, such as GABA aminotransferase.

Addresses: [1]Department of Molecular Biophysics and Biochemistry, Yale University, New Haven, CT 06520, USA and [2]The Howard Hughes Medical Institute, Yale University, New Haven, CT 06520, USA.

*Corresponding author.
E-mail: axel.brunger@yale.edu

Key words: gyrate atrophy, ornithine aminotransferase, pyridoxal -5′-phosphate, substrate recognition, suicide inhibitor, X-ray structure

Received: 30 May 1997
Revisions requested: 27 June 1997
Revisions received: 7 July 1997
Accepted: 9 July 1997

Structure 15 August 1997, 5:1067–1075
http://biomednet.com/elecref/0969212600501067

Introduction

Aminotransferases are enzymes that catalyze the transfer of amino groups from amino acids to oxoacids. Collectively, they make up a group of homologous proteins [1] that share a similar vitamin B6-dependent mechanism. Ornithine aminotransferase (OAT, L-ornithine:2-oxoacid aminotransferase, EC 2.6.1.13) is a 45 kDa enzyme that catalyzes the transfer of the δ-amino group of L-ornithine to 2-oxoglutarate. The metabolic importance of OAT in regulating ornithine levels is underscored by the fact that deficiencies of the enzyme in humans result in hyperornithinemia, a condition that leads to gyrate atrophy of the choroid and retina which progressively causes blindness [2]. OAT is distinct from other aminotransferases, for which there is detailed structural and mechanistic information [3], in that it is specific for an amino group other than the carboxyl bearing α-amino group. Another member of the same subgroup of aminotransferases [4] is γ-aminobutyric acid aminotransferase (GABA-AT), an enzyme whose substrate is the brain's major inhibitory neurotransmitter. In addition to having high sequence homology, OAT and GABA-AT also share a common inhibitory mechanism [5], a fact that has complicated efforts to design inhibitors that selectively inactivate GABA-AT [6].

The transamination cycle in pyridoxal phosphate (PLP)-dependent enzymes can be divided into two half reactions. In the case of OAT, the first half reaction begins with ornithine binding in the active site where the Schiff-base linkage between the PLP cofactor and Lys292 is transferred to the δ-amino group of ornithine. Following deprotonation and hydrolysis at the δ-carbon of ornithine, glutamate-γ–semialdehyde is released, leaving the cofactor with an amino group bound to it as pyridoxamine-5′-phosphate (PMP). The second half reaction is a reversal of the first, with 2-oxoglutarate binding and reacting with the PMP cofactor, yielding L-glutamic acid and regenerating the Schiff base between the PLP and active site Lys292. In order to learn more about the

Figure 1

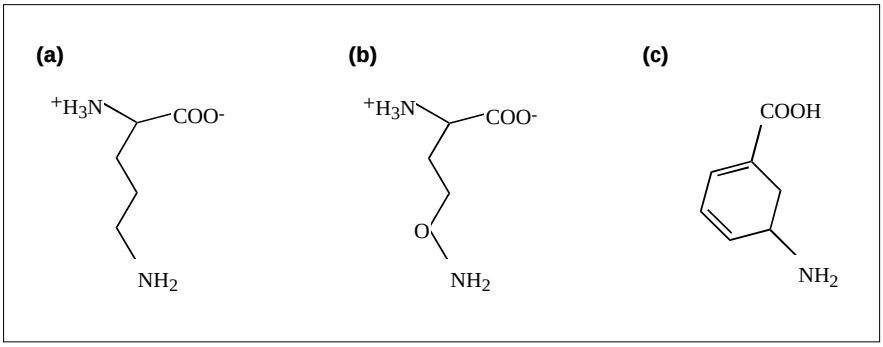

Substrate and inhibitor chemical structures. Chemical structures of (a) L-Ornithine, (b) α-amino-γ-amino-oxybutyric acid (L-canaline) and (c) 5-amino-1,3,-cyclohexadienyl carboxylic acid (gabaculine).

structural basis for substrate recognition, it is useful to capture the enzyme in a stable intermediate state within the transamination cycle for the purposes of crystallographic analysis. Enzyme activated irreversible inhibitors are ideal for this purpose, because they function by a mechanism requiring partial catalytic turnover by the enzyme that leads to a stable dead-end intermediate.

Figure 2

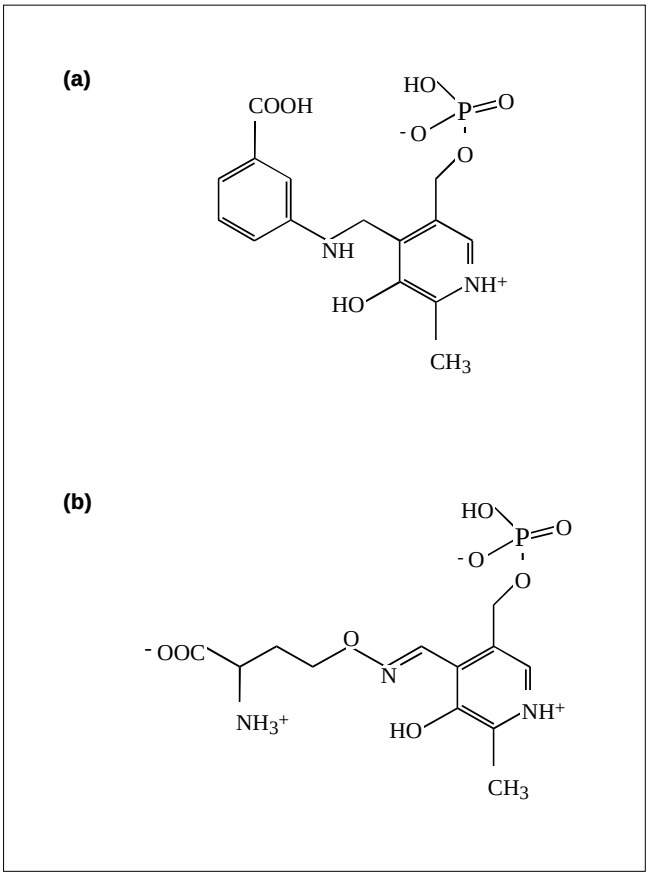

Irreversible inhibitor–cofactor intermediate structures. Chemical structures of the irreversible intermediates generated upon binding of (a) gabaculine and (b) L-canaline to pyridoxal phosphate.

L-gabaculine (5-amino-1,3-cyclohexadienyl carboxylic acid) is a naturally occurring irreversible inhibitor of GABA-AT [7] (Figure 1). Because of the nearly identical mechanisms of transamination between OAT and GABA-AT, as well as the similarity of their substrates, it was found that gabaculine is an equally potent irreversible inhibitor of OAT [5]. Gabaculine's mechanism of action is somewhat unique in that it involves generation of an aromatic compound. After gabaculine binds to the active site of OAT and forms a Schiff base with the PLP cofactor, a hydrogen is removed from the imino bearing carbon of the inhibitor, as it would be from the natural substrate ornithine. In the case of gabaculine, however, hydrogen abstraction at the β-carbon position leads to an unstable intermediate that is converted to m-carboxyphenylpyridoxamine phosphate, an extremely stable and irreversible aromatic modification of the cofactor [7] (Figure 2).

A structural analogue of L-ornithine, L-canaline (α-amino-γ–amino-oxybutyric acid), has also been shown to be a strong inhibitor of OAT [8] (Figure 1). It inhibits the enzyme by forming a stable oxime with the PLP cofactor via its γ-aminooxy group (Figure 2b). Although L-canaline is a reversible competitive inhibitor of aspartate aminotransferase, it is irreversible with respect to OAT. This specificity is thought to be the result of the similar interactions that ornithine and L-canaline make between their α-amino and carboxyl groups and the active site of OAT [9]. The actual residues involved in these contacts, however, until now have not been known.

We present here the crystal structures of OAT in complex with gabaculine and L-canaline refined to 2.3 Å, allowing detailed analysis of the specific residues involved in inhibitor binding. In the case of gabaculine, we find that aromatic–aromatic interactions between active-site residues and the bound inhibitor play a significant role in

the inhibitor's potency. The L-canaline complex allowed the specific residues involved in coordinating with the α-amino and carboxyl groups to be determined. The role of these active-site residues in the recognition of the natural substrate, L-ornithine, and their correlation with two inherited mutations in OAT that result in gyrate atrophy in humans are also discussed.

Results and discussion

Structure determination

Complexes of ornithine aminotransferase both with L-canaline and gabaculine were obtained by co-crystallization of protein that had been pre-incubated with inhibitor. Diffraction data, using glycerol as cryo-protectant, were collected at 110K on each respective protein–inhibitor complex (Table 1). Both complexes crystallized in the same space group ($P3_221$) and has similar overall unit cell dimensions as native OAT crystals [10]. The co-crystal data were phased by difference Fourier techniques using the structure of native OAT, solved to 2.5 Å (BWS, M Hennig, E Hohenester, T Schirmer and JN Janionius, unpublished data). The asymmetric unit in both native and inhibitor-bound complex crystals consists of three OAT protomers (one and a half dimers) related by a noncrystallographic threefold axis [11]. An initial model consisting of three OAT protomers, with no PLP or inhibitor atoms, was subjected to rigid-body minimization and torsion-angle dynamics [12] against the inhibitor-bound data. F_o–F_c difference maps using phases from this ligand-free model, clearly showed the presence of inhibitor and cofactor density within the active site of both the OAT–gabaculine and OAT–L-canaline complexes (Figure 3). After the addition of inhibitor and cofactor atoms, several rounds of rebuilding into composite annealed omit maps was carried out, which allowed misplaced sidechain and backbone atoms to be properly positioned. Statistics for the final models are given in Table 2. In the following sections, all structural analysis and calculations were made using only one of the three protomers in the asymmetric unit.

Table 1

Data collection statistics.

Inhibitor	Gabaculine	Canaline
X-ray source, λ (Å)	CHESS, 0.9417	CHESS, 0.9417
Space group	P3(2)21	P3(2)21
Unit cell a,b,c (Å)	115.0, 115.0, 185.7	115.9, 115.9, 185.7
Resolution range (Å)	50.0–2.3	50.0–2.3
Unique reflections	57,010	56,813
R_{merge} (%)*	6.4 (17.1)	9.8 (18.2)
Completeness (%)	89.9 (80.1)	87.4 (66.3)
Redundancy	4.6 (2.6)	4.3 (3.1)

*$R_{merge} = \Sigma_{hkl}\Sigma_i | < I(hkl) > - I(hkl)_i | / \Sigma_{hkl} < I(hkl) >$, where $I(hkl)_i$ is the measured diffraction intensity and $< I(hkl) >$ equals the mean value of intensity. Values indicated in parentheses are for the highest resolution shell (2.4–2.3 Å).

Figure 3

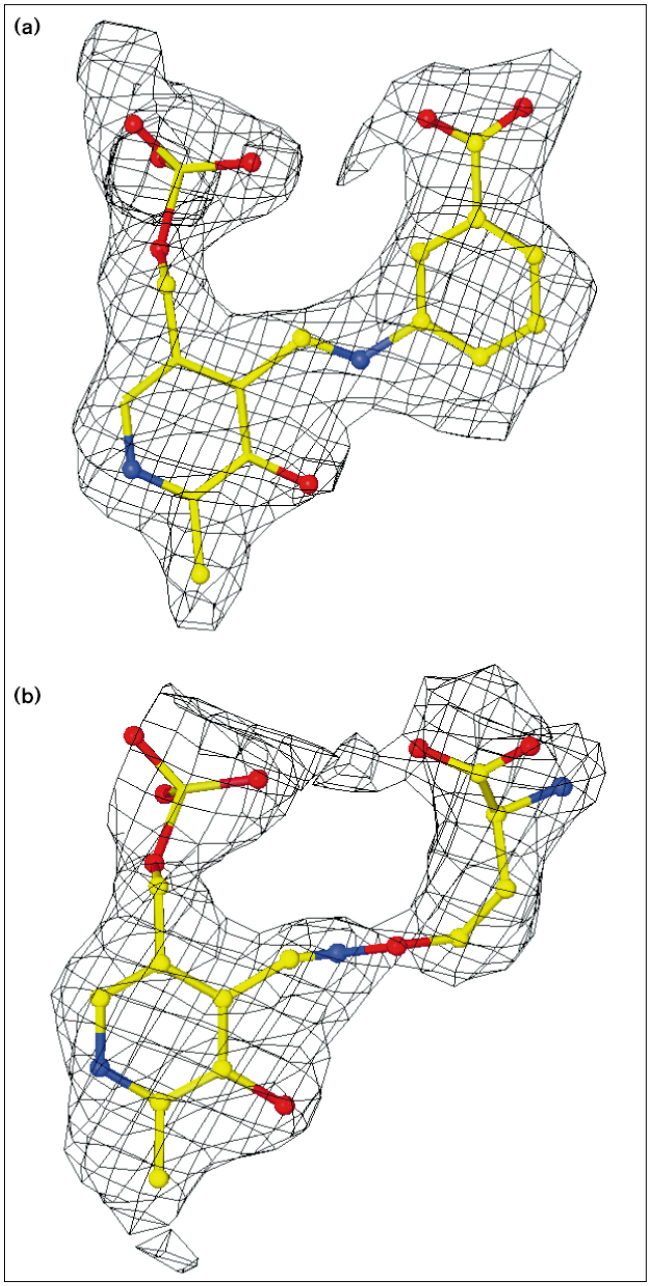

Omit density map. F_{obs}–F_{calc}(omit) density is shown contoured at 2σ, superimposed on the final refined coordinates of the PLP cofactor and (a) gabaculine inhibitor or (b) L-canaline. Calculated structure factors used for the map calculation were obtained from a preliminary model in which the inhibitor and PLP cofactor were omitted from refinement. Atoms are shown in standard colors.

Overall structure and domain movement

A single asymmetric unit in the OAT–inhibitor complex structures consists of one and a half dimers of OAT related by a threefold noncrystallographic symmetry. Although the protein is active as a dimer, each monomer has its own

Table 2

Refinement statistics*.

Inhibitor	Gabaculine	Canaline
Resolution range (Å)	50.0–2.3 (2.4–2.3)	50.0–2.3 (2.4–2.3)
Reflections F > 2σ	52,218 (5123)	54,425 (4654)
Number of atoms (non H)	9525	9525
Bulk solvent parameters		
k_{sol} (electrons / Å^3)	0.4324	0.3735
B_{sol} (Å^2)	44.34	47.44
R_{free} (%)†	23.48 (28.88)	23.66 (29.55)
R_{cryst}(%)†	20.63 (25.81)	20.99 (26.16)
Number of waters	329	276
Rmsd bond length (Å)	0.007	0.007
Rmsd bond angle (°)	1.320	1.322
Average B factor (Å^2)		
water atoms	24.04	31.29
protein atoms	22.5	28.71
Ramachandran plot		
most favored regions (%)	85.5	86.2
allowed regions (%)	13.6	12.9

*Values indicated in parentheses are for the highest resolution shell (2.4–2.3 Å). †$R_{cryst} = \Sigma_{hkl} | |F_{obs}(hkl)|–k|F_{calc}(hkl)| | / \Sigma hkl |F_{obs}(hkl)|$; $R_{free} = R_{cryst}$ for a test set of reflections not used during refinement (10% for both complexes).

active site with numerous contacts between adjacent active sites in the dimer. Each OAT monomer can be subdivided into three domains — an N-terminal segment, a small C-terminal domain and a large PLP-binding domain. The active site of the enzyme is centered around the PLP cofactor, and it is located in the cleft between the large and small domains of the protein (Figure 4). This type of fold is common among several PLP-dependent enzymes, including dialkylglycine decarboxylase and aspartate aminotransferase [11]. It was of interest to this study whether OAT undergoes a significant conformational change upon ligand binding, similar to that observed for aspartate aminotransferase (AAT) in which a 13° rotation of the small C-terminal domain towards the large PLP-binding domain is observed [13]. Superposition of the refined Cα coordinates of each inhibitor-bound complex on the ligand-free native structure reveals no significant bulk domain movements. The OAT–L-canaline complex does exhibit a slightly more open conformation with respect to the gabaculine-bound complex, however. In order to quantitate the extent of domain closure in the gabaculine complex, a difference distance matrix analysis was employed [14]. In such an analysis, a matrix containing all the intra-atomic Cα distances of a protein is subtracted from an identical matrix of an identical or related protein. This type of comparison is independent of the relative rotation or translation of the two coordinate sets and thus is not biased by the method in which the two structures are overlaid. The final plot of subtracted matrices gives the actual distance that the α-carbon of each residue has moved in relation to every other residue. The difference distance matrix plot between the canaline- and gabaculine-bound OAT structures (Figure 5), suggests that changes in Cα positions between the two structures occur mainly in three regions that correspond to the three domains of the enzyme: residues 38–116, residues 117–342 and residues 343–438. In both complexes, there is no change in the Cα positions between residues belonging to the same domain (intradomain movement, diagonal

Figure 4

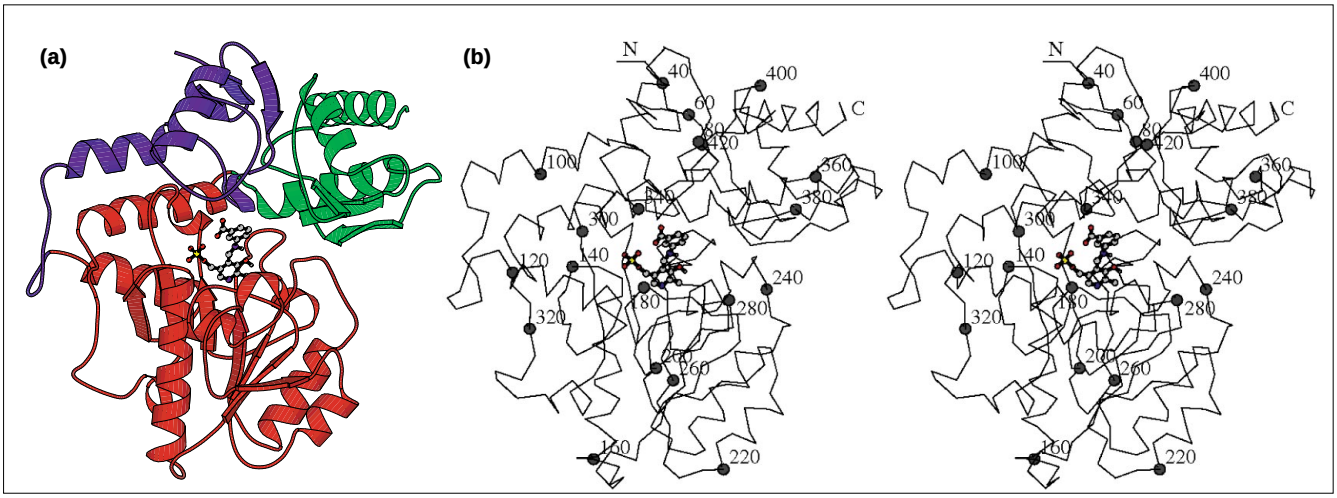

Overall structure and inhibitor-binding cleft. (a) Ribbon diagram of the OAT–gabaculine complex. OAT is colored with respect to each of its three domains, the N-terminal domain (blue), PLP-binding domain (red) and the C-terminal domain (green). The gabaculine–PLP cofactor complex, which resides in a cleft between the three domains, is shown in ball-and-stick representation (standard colors). (b) Stereo pair of the α-carbon trace of the OAT–gabaculine complex. Cα positions are labeled every twenty residues. (Figures prepared using MOLSCRIPT version 1.4 [30].)

Figure 5

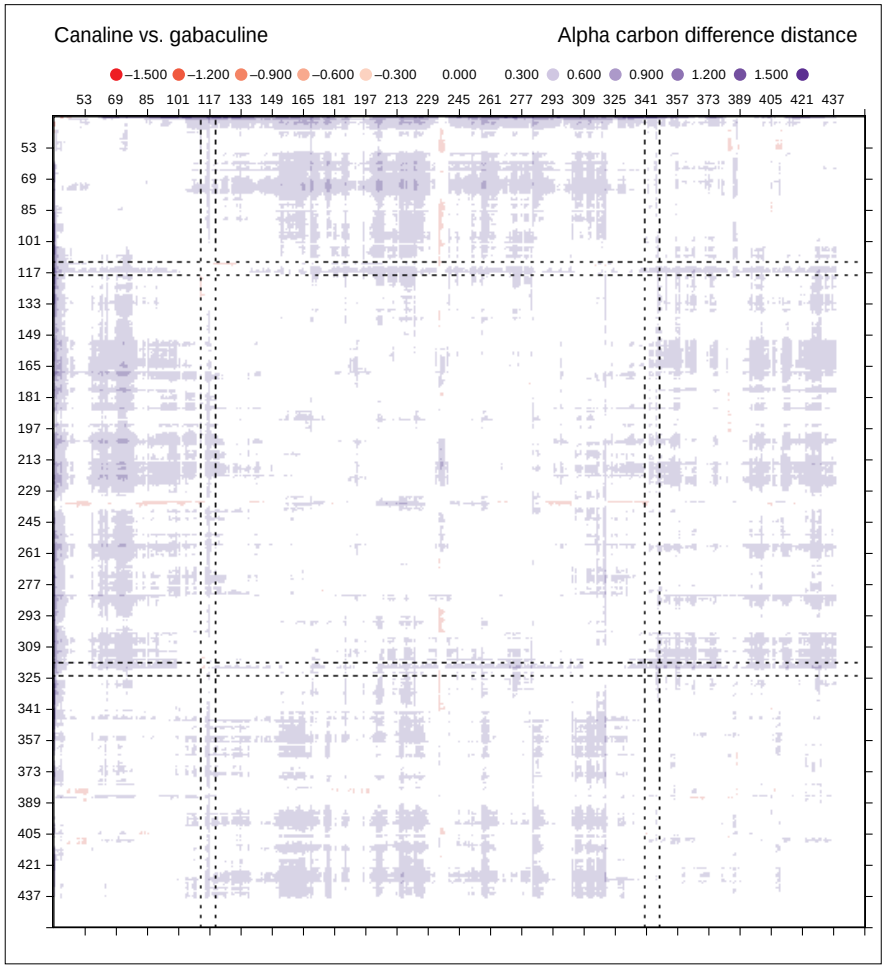

Difference distance matrix plot between the OAT–L-canaline and OAT–gabaculine complexes. The matrix calculation is over the Cα coordinates of residues 38–438 of each respective OAT–inhibitor complex. Positive differences, which correspond to a compacting of the gabaculine structure relative to the L-canaline structure, are given in increasing shades of purple. Negative differences are in red. Dotted lines indicate the domain boundaries. Boxes on the diagonal represent intradomain movement. Off-diagonal boxes represent interdomain movements. See text for interpretation. (Plot made using the DDMP program from the Center of Structural Biology, Yale University, New Haven, CT, USA.)

boxes in Figure 5). In contrast, the N- and C-terminal small domains appear to have moved slightly closer to the large PLP-binding domain in the gabaculine-bound structure (off-diagonal boxes in Figure 5). The approximate distance involved in the movement is shown to be between 0–1.2 Å. Although it is interesting that there is some flexibility in the relative orientation of the three domains of OAT, the distances involved are small and may be due to 'breathing' motions or packing effects resulting from differences in unit cell dimensions between the two complexes.

PLP-cofactor tilt

The conformation of the active site in inhibitor-free OAT is shown in Figure 6 (green). The PLP cofactor is covalently bound via a Schiff base to Lys292. Located above the PLP cofactor is a pocket that is flanked on three sides by aromatic residues, Tyr85, Phe177 and Tyr55. The substrate-binding site is in this pocket. Several residues from the adjacent monomer in the OAT dimer border the active site, including Thr322* (residues in the adjacent protomer will hereafter be indicated with an *). Several local sidechain conformational changes occur upon ligand binding that are consistent in both the gabaculine- and L-canaline-bound models. The most obvious changes occur in response to transfer of the internal Schiff base from Lys292 to the inhibitor. Once the Schiff base with the pyridoxal-5′-phosphate cofactor is broken, Lys292 is free to form a hydrogen bond with the sidechain of Thr322*. In addition, the PLP cofactor undergoes a rotation away from Lys292 and towards Phe177 (Figure 6, yellow). The degree of PLP rotation relative to the inhibitor-free structure differs between the two OAT–inhibitor complexes, with a 27¼ tilt induced in the gabaculine complex and a 21¼ rotation with the canaline complex. The 5′ phosphate and ring nitrogen of the cofactor remain relatively fixed, with the rotation induced mainly by torsions about the O5′–P and C5′–O5′ bonds. Phe177 which lies above the plane of the cofactor must also shift to accommodate the PLP movement. Specifically, its sidechain is forced to rotate about χ_1 by 10°, corresponding to 1.3 Å movement of the phenyl ring centroid.

Figure 6

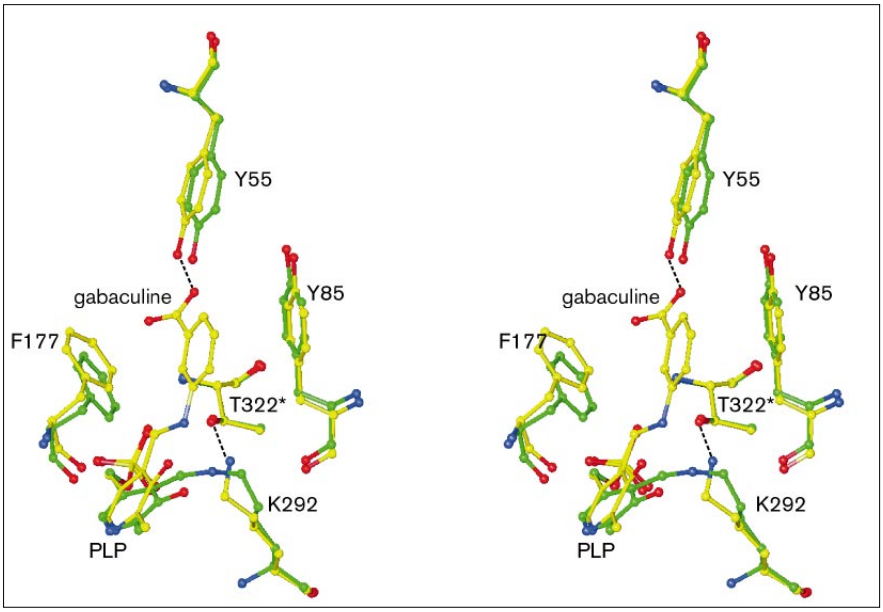

Stereoview of the conformational changes in OAT produced by gabaculine binding. Final model of the gabaculine-bound active site (yellow) superimposed on the ligand-free active site (green). Major conformational changes incurred upon inhibitor binding include a 27¼ rotation in PLP-cofactor tilt, and a corresponding 1.3 Å movement of Phe177. In addition, Lys292 forms a salt bridge with Thr322*, a residue located on an adjacent protomer in the OAT dimer. Hydrogen bonds are indicated with dashed lines. See text for discussion.

Gabaculine-binding mode: favorable aromatic interactions

In the ligand-bound form of OAT, the amine group of gabaculine is bound to the cofactor via a Schiff base, whereas one of the carboxyl oxygen atoms O7A forms a strong hydrogen bond with Tyr55 (Figure 6). Two interactions occur between the inhibitor carboxylate head group and residues in the adjacent monomer — a weak hydrogen bond between the backbone amide hydrogen of Ser321* and the other carboxyl oxygen atom O7 of the inhibitor (shown in Figure 7a) and a water mediated linkage between carboxyl oxygen O7A and the backbone amide of Arg113* (not shown). Hydrogen bonds between the carboxyl group of gabaculine and active-site residues help to position the inhibitor properly for Schiff-base formation with the PLP. Although the carboxyl head is the only functional group that gabaculine presents to the active site, the OAT–gabaculine crystal structure reveals an additional important interaction. Hydrogen abstraction from the bound inhibitor occurs at the carbon position adjacent to the Schiff base, which is analogous to that undergone by the natural substrate, ornithine. When gabaculine is bound, however, a second hydrogen abstraction at the β-carbon position leads to formation of an aromatic intermediate, m-carboxyphenyl pyridoxamine phosphate (mCPP) (Figure 2a) [15]. The structural basis for the strong binding of mCPP is evident from the residues that border the substrate binding pocket. Tyr85 is stacked in a near parallel fashion approximately 4.1 Å above the plane of the intermediate, whereas Phe177 is stacked at a nearly orthogonal angle on the opposite side of the intermediate, such that there is a distance of 5.2 Å between the ring centers of Phe177 and the inhibitor (Figure 7a). Favorable interactions such as these between aromatic protein residues are well documented, with a preferential distance between aromatic ring centers being 4.5–7 Å and relative angle between ring planes approaching 90° [16]. Monte Carlo simulations of benzene predict the tilted T arrangement and the parallel stacked and displaced arrangement to be two favorable conformations for benzene dimers, with interaction energies of –2.31 and –2.15 kcal/mol respectively [17]. These predicted conformations are very similar to the observed arrangements between Tyr85, Phe177 and the aromatic gabaculine intermediate in the crystal structure of OAT–gabaculine. The expected contribution to binding energy of approximately 4 kcal/mol that is donated by aromatic–aromatic interactions with active-site residues, provides the structural basis for why the OAT-catalyzed conversion of non-aromatic gabaculine to mCPP produces a dead-end irreversible intermediate.

Canaline binding: Arg180 and Tyr55

Although L-Canaline binds in the same pocket as gabaculine, it presents different functional groups to the active site. Like the natural substrate L-ornithine, L-canaline offers both an α-amino and a carboxyl group that are recognized by the enzyme. In the OAT–canaline crystal structure, the inhibitor carboxyl group coordinates with Arg180 and the backbone amide hydrogen of Ser321* (Figure 7b). The α-amino group of canaline forms a strong hydrogen bond with Tyr55, the same residue that bonds to the carboxyl group of the inhibitor in the OAT–gabaculine complex structure. No conformational change in the backbone of the enzyme is required to position these residues in the optimal orientation for coordination with

Figure 7

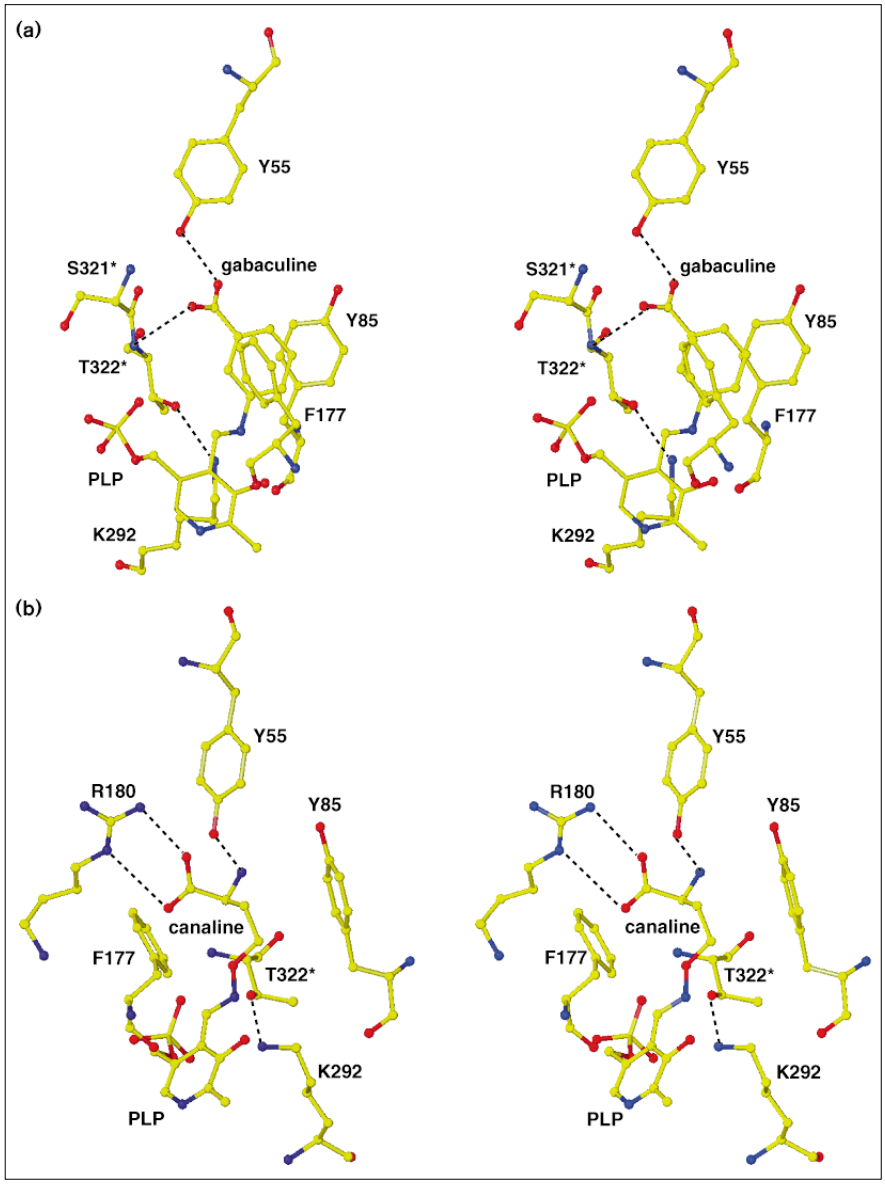

Stereoview of the inhibitor-bound active sites. (a) Gabaculine and (b) L-canaline are covalently bound to the PLP cofactor within the active site of OAT. Residues marked with * are located on an adjacent protomer in the OAT dimer. Hydrogen bonds are indicated with dashed lines. Of particular interest in (a) is the aromatic 'sandwich' made by residues Tyr85 and Phe177 around the aromatic gabaculine inhibitor. The active-site residues involved in hydrogen bonding to the carboxylate and amino groups of L-canaline are shown in (b). Both of these residues, Tyr55 and Arg180, are found to be among those mutated in patients suffering from gyrate atrophy, see text for discussion.

the inhibitor. The γ-aminooxy group of canaline is bound to the aldehyde position of the PLP cofactor via a stable oxime. The effect of this inhibitor on other aminotransferases has been studied and, in particular, it was found that L-canaline is a reversible non-competitive inhibitor of aspartate aminotransferase (AAT) [9]. The specificity of L-canaline as an irreversible inhibitor for OAT is a direct result of its similarity to ornithine. The active site of OAT, which has evolved to be selective for the δ-amino group, requires a strong coordination site to sequester the more reactive α-amino group and the adjacent carboxyl. In its inhibition of OAT, L-canaline takes advantage of these specific contacts. Oxime formation alone by canaline is not sufficient to cause irreversible inhibition of AAT. Oxime formation, in cooperation with specific contacts to Tyr55 and Arg180, make canaline inhibition of OAT irreversible.

Arg180 and Tyr55: implications for L-ornithine

The orientation of canaline in the active site of OAT, as well as the inhibitor's similarity to the natural substrate ornithine, implicate Tyr55 and Arg180 as the residues involved in positioning ornithine in the active site for specific transamination at the δ position. The role of Tyr55 and Arg180 as active site residues that are essential for substrate turnover is supported by genetic evidence gathered from humans suffering from gyrate atrophy. Gyrate atrophy of the choroid and retina, an inherited disease in humans characterized by elevated ornithine levels, has been shown

to be caused by deficiencies in OAT [2]. Sequence analysis of the OAT genes from patients with gyrate atrophy revealed 21 different mutant OAT alleles, 18 of which result in single amino acid changes in the enzyme [18].

Both Tyr55 and Arg180 are found to be mutated in patients suffering from gyrate atrophy. The observed phenotype of the two mutations, Tyr55→His and Arg180→hr, were tested in terms of mRNA expression levels and antigen response. Although the phenotype of the Tyr55→His mutation could not be determined due to compound heterozygosity, the Arg180→Thr mutant exhibited no change in mRNA levels and was one of only two mutations that abolished enzyme activity and exhibited no change in antigen response [18]. On the basis of the OAT–inhibitor complex structures, we conclude that the Tyr55His and Arg180Thr mutations may alter the affinity for substrate by disrupting the specific contacts that are necessary to position ornithine in the active site. These mutations would not prohibit binding of ornithine, as the substituted residues do not cause steric clashes, but instead they would affect the binding affinity by disrupting hydrogen bonds required to position the substrate.

Biological implications

Ornithine aminotransferase (OAT) catalyzes a reaction in the pathway that interconverts ornithine and proline, and also serves to connect the urea and citric acid cycles. Loss of OAT function in humans produces elevated levels of ornithine that can lead to gyrate atrophy (GA) of the choroid and retina, an inherited disease that results in blindness [2]. OAT is in the same subgroup as some other aminotransferases that also have key metabolic roles. This subgroup includes γ-aminobutyric acid aminotransferase (GABA-AT), an enzyme whose substrate is the brain's major inhibitory neurotransmitter, and glutamate-1-semialdehyde aminotransferase (GSA-AT), an essential enzyme in the tetrapyrrole synthesis pathway in plants. It is therefore of interest to learn more about the mechanism of enzymes in this subgroup and, in particular, identify the residues that are involved in substrate binding. Because loss of OAT function results in disease in humans, the enzyme is not a focus for rational inhibitor design. GABA-AT and GSA-AT, which are homologous to OAT, however, are targets for selective inactivation. Therefore, any information on the mechanism of inhibition with respect to OAT is relevant to rational drug design efforts on these other more attractive targets.

The inhibitor compounds, L-canaline and gabaculine, co-crystallized with OAT in this study, mimic the natural substrate well enough to bind to the active site of the enzyme and undergo the first steps of the transamination reaction. Unlike ornithine, however, they produce irreversible covalent intermediates with the PLP cofactor (bound in the OAT active site) that cripple the enzyme. Because L-canaline is virtually identical to ornithine, the structure presented here provides information on the specific residues in the active site that are involved in substrate recognition. In particular, the OAT–L-canaline complex reveals two residues, Tyr55 and Arg180, which donate the specific contacts necessary to position ornithine in the active site. These same residues have been found to be mutated in patients suffering from GA [18]. The structure presented here indicates that the mutated OAT in GA would be unable to bind the substrate ornithine, resulting in no enzymatic turnover.

GABA-AT and GSA-AT have a high sequence homology with OAT and are inactivated by common inhibitors, one of which is gabaculine. The mechanism by which this inhibitor operates has been well documented [5,7,15], and it proceeds by generating a stable aromatic intermediate. The crystal structure of OAT in complex with gabaculine provides the first structural evidence that the potency of the inhibitor is due to favorable aromatic–aromatic interactions with active-site residues. In particular, we see two aromatic residues, Tyr85 and Phe177, that sandwich the bound gabaculine. This type of interaction may play a role in modulating gabaculine's binding affinity in these related aminotransferases, and thus may be useful for future structure-based drug design efforts.

Materials and methods

Crystallization and data collection

Recombinant human ornithine aminotransferase was expressed in *Escherichia coli*, purified and crystallized under conditions similar to those described previously [10]. L-canaline and gabaculine were purchased from Sigma Chemical Co. and Fluka Chemical Corp., respectively. Purified OAT was pre-incubated with the appropriate inhibitor prior to crystallization at a 1:1 molar ratio. Crystals of each respective complex were obtained by the hanging-drop vapor diffusion method and grew to maximum size in about 1 weeks time. Following serial transfer to a mother liquor containing 25% glycerol, selected crystals were flash frozen in liquid propane and stored in liquid nitrogen until data collection. Diffraction data were collected on the A1 beam line at the Cornell High Energy Synchrotron Source (CHESS) at 110K. For each complex, data were recorded from a single crystal on a Princeton 2K CCD detector. Each data set was processed and scaled with DENZO and SCALEPACK [19]. For the OAT–L-canaline and OAT–gabaculine complex, data are, respectively, 89.9% and 87.4% complete to 2.3 Å (Table 1).

Structure determination and refinement

Crystals of both OAT–inhibitor complexes were of the same space group and had similar unit cell dimensions [10] as those of the native structure, which consists of three OAT monomers related by non-crystallographic symmetry (ncs) (BWS, M Hennig, E Hohenester, T Schirmer and JN Janionius, unpublished data). An initial model for the complex structures was obtained by rigid-body conjugate gradient refinement of the native monomers with the PLP cofactor removed, against the appropriate inhibitor bound data. All refinements, which used data with amplitudes greater than 2s and 10% of the observed reflections randomly removed for cross validation, were carried out with the programs X-PLOR [20] and the developmental program CNS (Crystallography and NMR System). Rigid-body minimization was followed by a simulated annealing refinement protocol [12,21] consisting of the following steps (ncs restraints [22] were applied to the three monomers throughout the refinement, as dictated by the free R value). Step 1:

initial 100 steps of conjugate-gradient minimization without the X-ray term but including harmonic restraints on the Ca coordinates in order to regularize the backbone geometry. Step 2: 1000 steps of constant temperature torsion-angle molecular dynamics [12] at 5000K. Step 3: 120 steps of all-atom molecular dynamics at 300K. Step 4: final 200 steps of Powell conjugate-gradient minimization. Steps 2 to 4 were carried out with the X-ray term included. The resulting model was used to compute sA [23] weighted and Fo–Fc maps, in which density for the PLP cofactor and respective inhibitor was clearly visible. The inhibitor and PLP cofactor atoms were built into the density of these maps using the program O [24]. These models were used to generate model-bias reduced composite annealed omit maps (see next section), into which minor sidechain and backbone errors, many of which were flagged by PROCHECK [25], were rebuilt. After repeating the refinement protocol described, restrained atomic B factor refinement was carried out with target deviations placed on atoms forming bonds and angles. Water molecules were automatically picked by searching difference maps for peaks greater than 2s that were between 2.2 and 4.0 Å away from a hydrogen-bond donor or acceptor. Two rounds of automatic water picking were carried out, first using 2Fo–Fc maps, and second against Fo–Fc maps. Each round included visual inspection of the electron density of each picked water, followed by positional and B-factor refinement. Water molecules with refined B factors greater than 60 Å2 were removed. Towards the later stages of refinement, a bulk solvent correction [26] was included which allowed all observed data to be used in refinement and map calculations. Throughout the course of model building and refinement, decrease in the crystallographic free R value [27] was used as a monitor for progress. The steps involved in refinement of the OAT–gabaculine and OAT–canaline complexes were carried out in an identical fashion. Statistics for the final models, which include a 'flat' bulk solvent correction [26], are given in Table 2.

Composite annealed omit maps

Composite annealed omit maps were used in the refinement process to guide model building. These maps are a combination of several techniques [22,28,29]. To create such a map, a region of the unit cell is first partitioned into cubic volumes covering the protein. The subset of atoms in a given volume plus a surrounding 'cushion' is deleted. The remaining 'neutral volume' atoms (those outside of the selected volume and surrounding cushion [28]) are refined (simulated annealing refinement starting at 400K followed by conjugate gradient minimization [29]) and used to compute a σ_A weighted [23] electron-density map of the omitted region. The complete map covering the protein is obtained by combining the partial maps generated from each omitted cube volume excluding the cushion. The width of each cubic volume for the maps computed here was set to 25 Å. A cushion of 5 Å surrounded each volume and harmonic positional restraints were applied to the atoms within a 2.0 Å buffer surrounding this cushion. Forty initial minimization steps followed by 100 steps of molecular dynamics at 400K and 20 steps of conjugate gradient minimization were performed for each cube refinement.

Accession numbers

The atomic coordinates for OAT in complex with L-canaline and gabaculine have been deposited in the Brookhaven Protein Data Bank with the code numbers 2can and 1gbn, respectively.

Acknowledgements

Supported in part by a grant from the National Science Foundation to ATB (BIR9514819). We thank Steve Ealick for providing access to the CHESS beamline A1. We thank Pat Fleming for assistance with difference distance matrix plotting and Paul Adams and Luke Rice for help with refinement and torsion angle dynamics. We also thank CG Kannangara for critical reading of the manuscript and Erin M Duffy for discussions regarding aromatic–aromatic binding interactions.

References

1. Alexander, F.W., Sandmeir, E. & Mehta, P.K. (1994). Evolutionary relationships among pyridoxal-5′-phosphate-dependent enzymes, Regio-specific α, β and γ families. *Eur. J. Biochem.* 219, 953–960.
2. Shih, V.E., Berson, E.L., Mandell, R. & Schmidt, S.Y. (1978). Ornithine ketoacid transaminase deficiency in gyrate atrophy of the choroid and retina. *Am. J. Hum. Genet.* 30, 174–179.
3. Metzler, C. (1985). *Transaminases*. John Wiley & Sons Inc, New York, USA.
4. Mehta, P.K., Hale, T.I. & Christen, P. (1993). Aminotransferases: demonstration of homology and division into evolutionary subgroups. *Eur. J. Biochem.* 214, 549–561.
5. Jung, M.J. & Seiler, N. (1978). Enzyme-activated irreversible inhibitors of L-ornithine:2-oxoacid aminotransferase. *J. Biol. Chem.* 253, 7431–7439.
6. John, R.A., Jones, E.D. & Fowler, L.J. (1979). Enzyme-induced inactivation of transaminases by acetylenic and vinyl analogues of 4-aminobutyrate. *Biochem. J.* 77, 721–728.
7. Rando. R.R. (1977). Mechanism of the irreversible inhibition of γ-aminobutyric acid-α-ketoglutaric acid transaminase by the neurotoxin gabaculine. *Biochemistry* 16, 4604–4610.
8. Rahailia, E.L., Kekomäki, M., Jänne, J., Raina, A. & Räihä, N.C.R. (1971). Inhibition of pyridoxal enzymes by L-canaline. *Biochim. Biophys. Acta.* 227, 337–343.
9. Kito, K., Sanada, Y. & Katunuma, N. (1978). Mode of inhibition of ornithine aminotransferase by L-canaline. *J. Biochem.* 83, 201–206.
10. Shen, B.W., Ramesh, V., Mueller, R., Hohoenester, E., Hennig, M. & Jansonius, J. (1994). Crystallization and preliminary X-ray diffraction studies of recombinant human ornithine aminotransferase. *J. Mol. Biol.* 24, 128–130.
11. Jansonius, J.N., *et al*., & Toney, M.D. (1994).Crystallographic studies on the vitamin B_6-assisted enzyme transamination reaction. In *Biochemistry of Vitamin B_6 and PQQ*. (Marino, G., Sannia G. & Bossa, F., eds), pp. 29–34, Birkhauser Verlag, Basel, Switzerland.
12. Rice, L.M. & Brünger, A.T. (1994). Torsion angle dynamics: reduced variable conformational sampling enhances crystallographic structure refinement. *Proteins* 19, 277–290.
13. Kirsch, J.F., Eichele, G., Ford, G.C., Vincent, M.G. & Jansonius, J. (1984). Mechanism of action of aspartate aminotransferase proposed on the basis of its spatial structure. *J. Mol. Biol.* 174, 497–525.
14. Kundrot, C.E. & Richards, F.M. (1988). Identification of structural motifs from protein coordinate data: secondary structure and first-level supersecondary structure. *Proteins* 3, 71–84.
15. Soper, T.S. & Manning, J.M. (1982). Inactivation of pyridoxal phosphate enzymes by gabaculine, correlation with enzymic exchange of B-protons. *J. Biol. Chem.* 257, 13930–13936.
16. Burley, S.K. & Petsko, G.A. (1985). Aromatic–aromatic interaction: a mechanism for protein structure stabilization. *Science* 229, 23–28.
17. Jorgenson, W.L. & Severance, D.L. (1990). Aromatic–aromatic interactions: free energy profiles for the benzene dimer in water, chloroform, and liquid benzene. *J. Am. Chem. Soc.* 112, 4768–4774.
18. Brody, L.C., *et al*., & Valle, D. (1992). Ornithine δ-aminotransferase mutations in gyrate atrophy, allelic heterogeneity and functional consequences. *J. Biol. Chem.* 267, 3302–3307.
19. Otwinowski, Z. (1993). Oscillation data reduction program. In *Data Collection and Processing: Proceedings of the CCP4 Study Weekend*. (Sawyer, L., Isaacs, N. & Bailey, S., eds), pp. 56–62, SERC Daresbury Laboratory, Warrington, UK.
20. Brünger, A.T., Kuriyan, J. & Karplus, M. (1987). Crystallographic R factor refinement by molecular dynamics. *Science* 235, 458–460.
21. Brünger, A.T. (1992). *X-PLOR, Version 3.1. A System for X-ray Crystallography and NMR*. Yale University, New Haven, CT, USA.
22. Weis, W.I., Brünger, A.T, Skehel, J.J. & Wiley, D.C. (1990). Refinement of the influenza virus haemagglutinin by simulated annealing. *J. Mol. Biol.* 221, 737–761.
23. Read, R.J. (1986). Improved fourier coefficients for maps using phases from partial structures with errors. *Acta Cryst. A* 42, 140–149.
24. Jones, T.A. & Kjeldgaard, M. (1993). *O Version 5.9, The Manual*. Uppsala University, Uppsala, Sweden.
25. Laskowski, R.A., MacArthur, M.W., Moss, D.S. & Thornton, J.M. (1993) PROCHECK: a program to check the sterochemical quality of protein structures. *J. Appl. Cryst.* 26, 283–291.
26. Jiang, J-S. & Brünger, A.T. (1994). Protein hydration observed by X-ray diffraction: solvation properties of penicillopepsin and neuraminidase crystal structures, *J. Mol. Biol.* 43, 100–115.
27. Brünger, A.T. (1992). The free R value: a novel statistical quantity for assessing the accuracy of crystal structures. *Nature* 355, 472–474.
28. Bhat, T.N (1988). Calculation of an OMIT map. *J. Appl. Cryst.* 21, 279–288.
29. Hodel, A., Kim, S-H. & Brünger, A.T. (1992). Model bias in macromolecular structures. *Acta Cryst. A* 48, 851–859.
30. Kraulis, P.J. (1991). MOLSCRIPT: a program to produce both detailed and schematic plots of protein structures. *J. Appl. Cryst.* 24, 946–950.